

Depth of Erosion Under Storm Conditions

John F.A. Sleath¹

Abstract

A model is presented for the dynamics of the mobile layer of sediment on the sea bed under sheet flow conditions. The Karman-Polhausen method is used to determine the thickness of the mobile layer, the scaling for velocity phase and amplitude, and the phase lead of the velocity at the bottom of the mobile layer. The model does not make use of constitutive equations such as those suggested by Bagnold (1956). Agreement between the predictions of the model and existing laboratory measurements is good.

1. Introduction

When a pipeline is trenched into the seabed it is important to know how far below the surface of the bed the sediment may be disturbed by the action of extreme waves or currents. One element in a calculation of this disturbance depth is the thickness of the mobile layer of sediment.

In oscillatory flow, the thickness δ_s of the mobile layer depends on the relative importance of the bed shear stress and the force due to the pressure gradient. When the pressure gradient term is small δ_s is also small and is determined by the magnitude of the Shields parameter. However, when the pressure gradient is no longer negligible δ_s increases rapidly. It is this situation which is of most concern when considering the stability of structures on or in the seabed. Unfortunately, the experimental measurements (see, for example, Horikawa et al, 1982, Sawamoto and Yamashita, 1986, Dick and Sleath, 1991, Asano, 1992, Ribberink and Al-Salem, 1994, 1995, Li and Sawamoto, 1995a, and Zala Flores and Sleath, 1998) show considerable scatter under these conditions.

Several theoretical models have been proposed for the fluid/sediment motion in mobile layers in oscillatory flow (Bakker and Van Kesteren, 1986, Asano, 1990, Nadaoka and Yagi, 1990, Dibajnia and Watanabe, 1992, Li and Sawamoto, 1995b, Kaczmarek et al, 1995, Ono et al, 1996, Katori et al, 1996). Unfortunately, here too, there is significant disagreement between the predictions of the various models when

¹Reader, Dept. of Engrg., Cambridge Univ., Trumpington Street, Cambridge, CB2 1PZ, UK.
FAX: +44 1223 332662, e-mail: jfas@eng.cam.ac.uk

δ_s is large. Part of the problem is that some models assume quasi-steady relationships for sediment transport rate, etc, and are consequently most relevant to the situation where δ_s is small and pressure gradient and inertia terms may be neglected. Others, make use of constitutive equations, such as those of Bagnold (1956), whose reliability in oscillatory flow is uncertain.

The aim of the present paper is to re-examine this question using the well-known Karman-Polhausen method (see, for example, Schlichting, 1979). This method has been shown to give good results in a variety of applications. One of its advantages in the present case is that it allows us to choose a form of velocity profile which is known to be physically realistic when pressure gradient is significant and δ_s is large. Another advantage over the model presented by Sleath (1994) is that it is not necessary to make use of constitutive equations like those of Bagnold (1956).

Only oscillatory flow will be considered here. Also, since the main objective is to examine the mobile layer under extreme wave conditions, the discussion will be limited to flat beds, i.e. sheet flow.

2. The present model

A first step in the Karman-Polhausen method is to select a generalized velocity profile with sufficient disposable constants to ensure a good fit to the unknown real profile. For present purposes we take the horizontal component of velocity to be given by

for $K_1 y \leq 1$

$$u = U_0 K_1 y R \left\{ e^{i(\omega t + \phi - K_2 y)} \right\}, \quad (1)$$

for $K_1 y > 1$

$$u = U_0 R \left\{ e^{i\omega t} \right\} \quad (2)$$

where $R \{ \}$ indicates the real part, U_0 is the amplitude of the fluid velocity in the free stream above the bed, ω is the angular frequency, K_1, K_2, ϕ are coefficients which remain to be determined and y is measured vertically up from the still bed level. This form of velocity profile was shown by Dick and Sleath (1991) to give good agreement with their measurements.

The Karman-Polhausen method involves integration of the momentum equation. In the present case we integrate between the still bed level ($y=0$) and the initial bed height ($y=\delta_s$) which we define as the level of the crests of the grains on the surface when the flow is stationary and all sediment has settled on the bed. Thus

$$\delta_s = \frac{1}{C_*} \int_0^{\infty} C dy \quad (3)$$

where C is the concentration of sediment at any height y and C_* is the limiting value of C for a stationary bed.

To start with we consider only the situation where $K_1 \delta_s \leq 1$. If we denote the amplitude of u at $y=\delta_s$ by U_m we have

$$K_1 = \frac{1}{\delta_s} \frac{U_m}{U_0}. \quad (4)$$

Also, if there is to be no discontinuity in phase at $K_1 y = 1$ we must have

$$K_2 = \frac{\phi}{\delta_s} \frac{U_m}{U_0} \quad (5)$$

We take the shear stress at $y = \delta_s$ to be

$$\tau = \tau_0 R \left\{ e^{i(\alpha x + \theta)} \right\}, \quad (6)$$

where τ_0 and θ are constants. At the lower boundary ($y=0$)

$$(\tau)_{y=0} = \text{const } \mu \left(\frac{\partial u}{\partial y} \right)_{y=0} \quad (7)$$

where μ is dynamic viscosity. The constant in this equation is intended to allow for the fact that the effective viscosity is a function of C/C_* . We assume that it is a constant because C/C_* must reach some limiting value as $y \rightarrow 0$ and so effective viscosity must tend to a limit also.

If Eq (7) holds it follows from Eq(1) that we may also write

$$(\tau)_{y=0} = \tau_b R \left\{ e^{i(\alpha x + \phi)} \right\}. \quad (8)$$

The momentum equation is

$$\rho_m \frac{\partial u}{\partial t} = - \frac{\partial p}{\partial x} + \frac{\partial \tau}{\partial y}, \quad (9)$$

where ρ_m is the density of the fluid/sediment mixture. Outside the boundary layer at the bed it follows from Eqns (9) and (2) that

$$\frac{\partial p}{\partial x} = \rho U_0 \omega \sin \alpha x \quad (10)$$

where ρ is fluid density. Substituting in Eq (9) and integrating from $y=0$ to $y=\delta_s$ we have

$$\begin{aligned} \tau_0 e^{i(\alpha x + \theta)} - \tau_b e^{i(\alpha x + \phi)} &= \int_0^{\delta_s} \left(\rho_m \frac{\partial u}{\partial t} - i \rho U_0 \omega e^{i \alpha x} \right) dy \\ &= \frac{\rho_m U_0 \omega}{K_1} \left[B^2 \left(i - \frac{U_m}{B U_0} \right) e^{i(\alpha x + \phi(1 - U_m/U_0))} - i B^2 e^{i(\alpha x + \phi)} - \frac{i U_m}{U_0} \frac{\rho}{\rho_m} e^{i \alpha x} \right] \end{aligned} \quad (11)$$

where

$$B = \frac{K_1}{K_2} = \frac{1}{\phi}, \tag{12}$$

and we have assumed ρ_m to be constant throughout the mobile layer. Dividing through by $\exp(i(\omega t + \theta))$ and then equating real and imaginary parts of Eq (11) we find

$$\tan(\phi - \theta) = \frac{\cos(\phi - \theta) - \cos \gamma + \frac{U_m \phi}{U_0} \sin \gamma + \frac{U_m}{U_0} \frac{\rho}{\rho_m} \phi^2 \cos \theta}{\frac{\tau_0 K_1 \phi^2}{\rho_m U_0 \omega} - \sin(\phi - \theta) + \sin \gamma + \frac{U_m \phi}{U_0} \cos \gamma + \frac{U_m}{U_0} \frac{\rho}{\rho_m} \phi^2 \sin \theta} \tag{13}$$

and

$$\tau_b \sin(\phi - \theta) = \frac{\rho_m U_0 \omega}{K_1 \phi^2} \left[\cos(\phi - \theta) - \cos \gamma + \frac{U_m \phi}{U_0} \sin \gamma + \frac{U_m}{U_0} \frac{\rho}{\rho_m} \phi^2 \cos \theta \right] \tag{14}$$

where

$$\gamma = \phi \left(1 - \frac{U_m}{U_0} \right) - \theta \tag{15}$$

As mentioned earlier, the flow may be treated as quasi-steady when the pressure gradient and inertia terms are negligible, i.e when the parameter

$$S = \frac{\rho U_0 \omega}{(\rho_s - \rho) g} \tag{16}$$

is small. Here ρ_s is the density of the sediment. Under these conditions the normal stress due to grain/grain interactions supports the sediment above at each instant in the wave cycle. If the ratio of shear stress to normal stress at the bottom of the mobile layer is some constant K (as shown by Bagnold, 1954, Savage and McKeown, 1983, Hanes and Inman, 1985)

$$\tau_b = K(\rho_s - \rho) g C_s \delta_s \tag{17}$$

where δ_s is, under these conditions, the maximum thickness of the mobile layer during the course of a half cycle.

Dick and Sleath (1991) showed that δ_s remains nearly constant during the cycle at larger values of S . Under these circumstances we assume that it is the average value of the normal stress over a half cycle which supports the sediment above. Thus

$$\tau_b \frac{2}{\pi} = K(\rho_s - \rho) g C_s \delta_s \quad (18)$$

Substituting from Eq (14) into Eq (18)

$$\frac{\pi}{2} \sin(\phi - \theta) K C_s = \frac{\rho U_0 \omega}{(\rho_s - \rho) g} \frac{\rho_m}{\rho K_1 \delta_s \phi^2} \left[\cos(\phi - \theta) - \cos \gamma + \frac{U_m \phi}{U_0} \sin \gamma + \frac{U_m}{U_0} \frac{\rho}{\rho_m} \phi^2 \cos \theta \right] \quad (19)$$

(This is the expression for high S . The expression for low S is the same with the leading $\pi/2$ deleted).

Finally, from Eqns (1), (7) and (18),

$$\text{const } \mu K_1 U_0 = \frac{\pi}{2} K(\rho_s - \rho) g C_s \delta_s \quad (20)$$

Eqns (4), (13), (19) and (20) allow us to determine U_m/U_0 , $\rho U_0 \omega \delta_s / \tau_0$ and ϕ for any value of $\rho U_0 \omega / (\rho_s - \rho) g$ provided we know the flow conditions, the sediment properties, and the value of the constant in Eqn (7).

So far, we have considered only the case where $K_1 \delta_s \leq 1$. This is the situation which applies at small to medium values of S . At large values of S we need to consider $K_1 \delta_s > 1$. This involves extending the integration in Eq (11) into the region covered by Eq (2). The extension is straightforward and, consequently, will not be discussed further here.

3. Comparison with experiment at large S

The main aim of the present paper is to investigate trends at high values of S . Consequently, we will compare the computed curves with the measurements of Dick and Sleath (1991) and Zala Flores and Sleath (1998) for acrylic sediment of density 1141 kg/m^3 and median diameter 0.7 mm .

The best fit of the experimental data for mobile layer thickness to the computed curves gives a value for the constant in Eq (7):

$$\text{const} = 14860 \quad (21)$$

Assuming this value to be correct, we can calculate curves for the various quantities of interest for given values of the parameter V defined as

$$V = f_w \frac{U_0}{(\omega V)^{1/2}} \quad (22)$$

where

$$f_w = \frac{\tau_0}{\frac{1}{2}\rho U_0^2} \tag{23}$$

is the friction factor calculated from Jonsson's (1963) curve for flat beds.

Fig. 1 shows how the ratio of the scaling factors K_1 / K_2 varies with the parameter $S = \rho U_0 \omega / (\rho_s - \rho)g$. Both theory and experiment show that the ratio is close to unity over a wide range of S , although the theory predicts a rise in K_1 / K_2 as $S \rightarrow 0$. The theoretical value of K_1 / K_2 at large S shows little dependence on the value chosen for the various constants.

The way in which the phase lead ϕ of the velocity at the bottom of the mobile layer varies with S is shown in Fig. 2. The parameter S is a measure of the importance of the pressure gradient terms in the equations of motion. As $S \rightarrow 0$, the

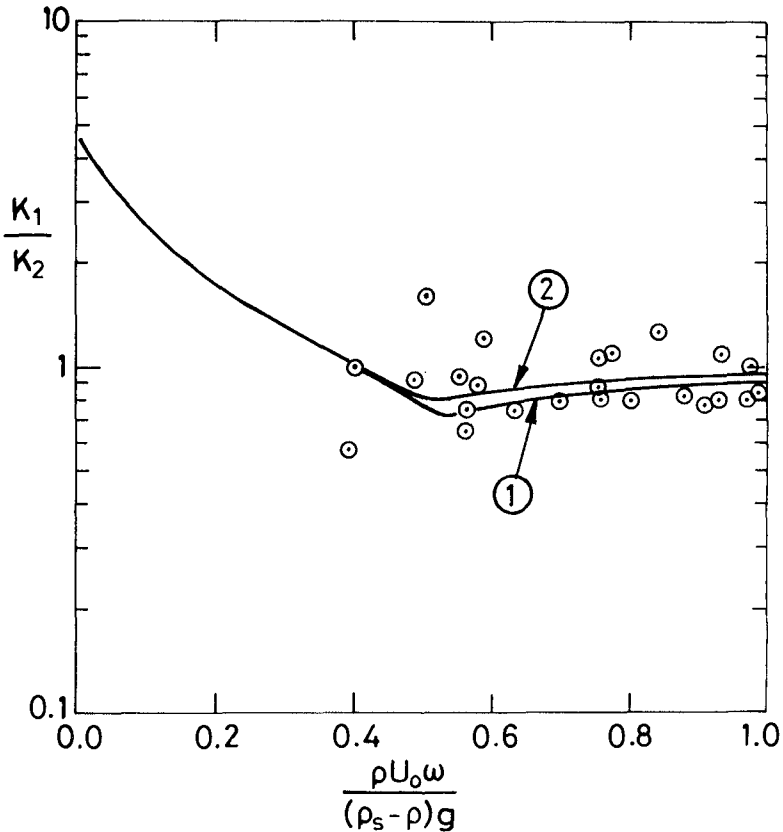


Fig.1 Variation of K_1 / K_2 with $\rho U_0 \omega / (\rho_s - \rho)g$ for the acrylic sediment of Dick and Sleath (1991). Curve 1, $V=10$; curve 2, $V=25$ (assuming $C_*K=0.35$, $\theta = 12.5^\circ$).

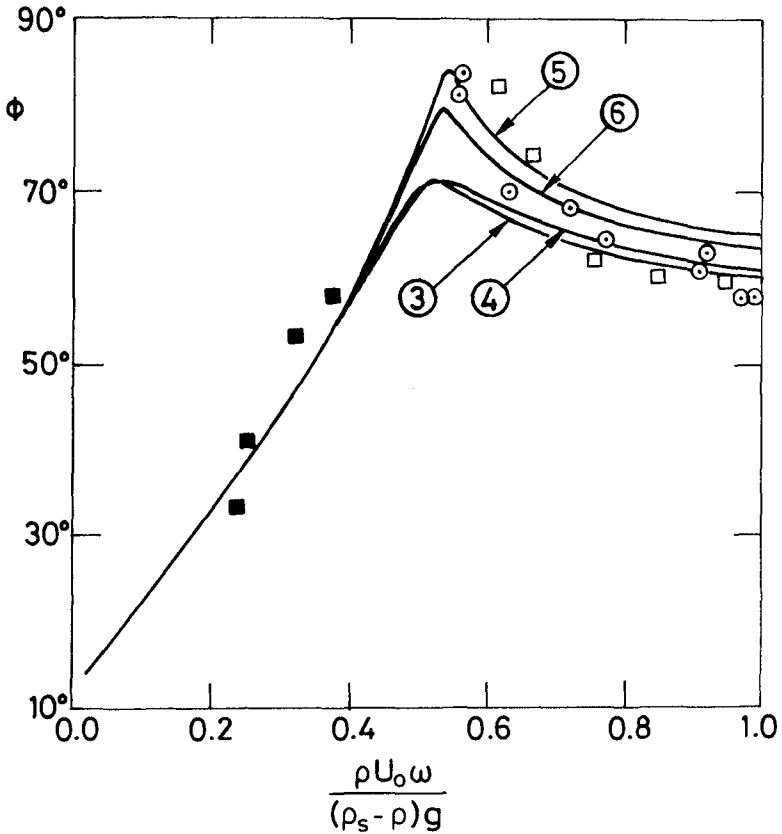


Fig.2 Variation of ϕ with $\rho U_0 \omega / (\rho_s - \rho) g$. Dick and Sleath (1991): \circ (acrylic). Zala Flores and Sleath (1998): \square (acrylic), \blacksquare (PVC). Curve 3, $V=25$; curve 5, $V=4$; curve 6, $V=10$; curve 4, inertial boundary condition with $I=0.8$, ($C_s K=0.35$, $\theta=12.5^\circ$ in each case).

pressure gradient terms become negligible and the flow is dominated by the shear stress acting on the upper surface of the mobile layer. Consequently, in this limit $\phi \rightarrow \theta$. As S increases from zero, pressure gradient becomes more important and the phase ϕ moves closer towards that of the pressure gradient. However, when S exceeds $C_s K$ the thickness of the mobile layer becomes much larger and consequently the inertia of the fluid/sediment mixture in the mobile layer becomes significant. This is why the value of ϕ falls at large S .

In Dick and Sleath's (1991) tests with acrylic sediment the values of V ranged from 6.8 at $S=0.55$ up to 18.5 at $S=0.96$. Consequently, the agreement between these tests and the computed curves in Fig. 2 is good. Zala Flores and Sleath's (1998) tests with acrylic sediment, which cover a similar range of values of S and V also show good agreement with the computed curves. This is more surprising since most of these

tests showed plug formation. It would appear that plug formation does not significantly modify the value of ϕ .

Fig. 2 also shows Zala Flores and Sleath's (1998) results for PVC granules. Once again there is good agreement with the trend of the computed curves even though we would expect the computations to be less reliable at small S .

In both Figs 1 and 2 the value of $C_s K$ has been taken as 0.35. An increase in $C_s K$ would move the computed curves bodily to the right and a decrease to the left. The value of 0.35 was chosen so that the maximum of the computed curves fell in approximately the right place in Fig. 2. The value of θ selected for the computations is typical of velocity measurements over rough beds. The computed curves were found to be relatively insensitive to the value chosen for θ .

It was suggested by Bagnold (1954) that under some conditions the component of shear stress due to grain/grain interactions is proportional to the square of the velocity gradient rather than directly proportional to it. He referred to this situation as the "inertial" regime. The interstitial component of shear stress at the bottom of the mobile layer would be relatively small in this situation and so Eq (7) would have to be replaced by an expression of the form

$$(\tau)_{y=0} = const \rho_s D^2 \left(\frac{\partial u}{\partial y} \right)_{y=0}^2 \tag{24}$$

where D is median grain size. Fig. 2 shows, for purposes of comparison, a curve computed with this inertial boundary condition instead of Eq (7). For this curve, the constant in Eq (24) has been taken equal to 125 and the parameter

$$I = f_w \left[\frac{a}{D} \right]^{2/3} \tag{25}$$

is equal to 0.8. Clearly, the use of an inertial boundary condition does not significantly change the general trend of the computed curves.

A quantity of great interest from the engineering point of view is the thickness δ_s of the mobile layer. At low values of S pressure gradient terms are unimportant and consequently δ_s is a function only of $\tau_0 / (\rho_s - \rho)g$. Sleath (1994) suggested, from comparison with experiment, that

$$\frac{\delta_s}{D} = 2.94 \frac{\tau_0}{(\rho_s - \rho)gD} \tag{26}$$

At high values of S it is the shear stress which is unimportant and, consequently, we expect the parameter $\beta\delta_s$ to be a function of S alone. Fig. 3 shows how the computed curves for $\beta\delta_s$ compare with the measurements of Dick and Sleath (1991) and Zala Flores and Sleath (1998) for acrylic sediment. We see that there are distinct curves for different values of V at low values of S but that at high values of S the various curves are almost identical. Dick and Sleath's (1991) results lie in the range $6.8 < V < 18.5$ so the agreement with the computed curves is good. The agreement with the experimental results of Zala Flores and Sleath (1998) is less good. This is probably because these tests showed plug formation. Under these conditions the assumption leading to Eq (18) is not correct.

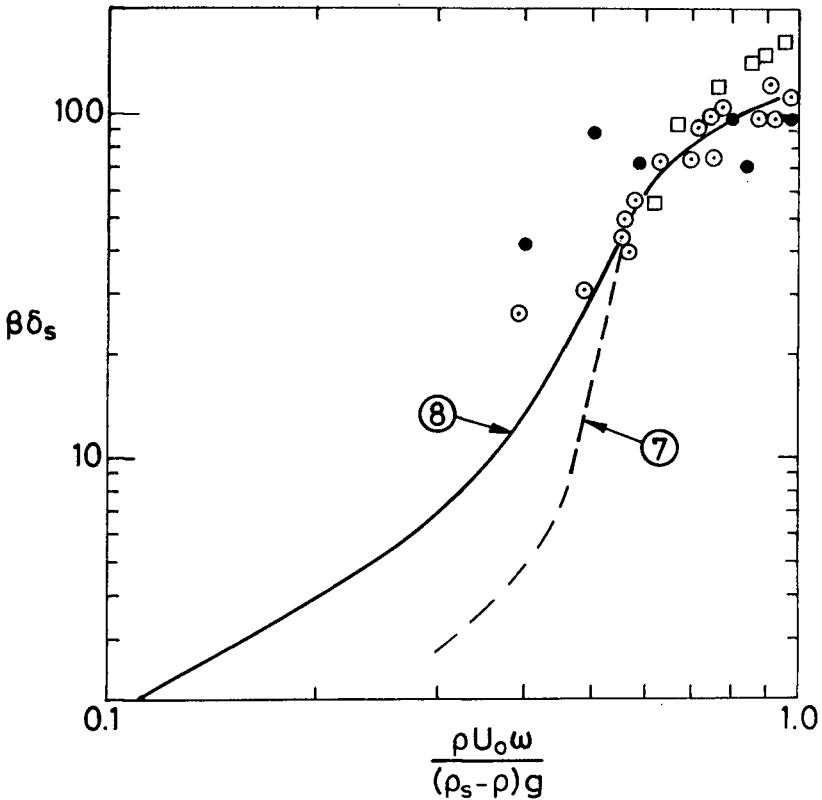


Fig.3 Variation of $\beta\delta_s$ with $\frac{\rho U_0 \omega}{(\rho_s - \rho)g}$. Dick and Sleath (1991): \circ (acrylic), \bullet (nylon). Zala Flores and Sleath (1998): \square (acrylic). Curve 7, $V=10$; curve 8, $V=25$, ($C_s K = 0.35$, $\theta = 12.5^\circ$ in each case).

Fig. 3 also shows Dick and Sleath's (1991) measurements with Nylon pellets of density 1137 kg/m^3 and median diameter 4.0 mm . The agreement with the computed curves is less good than for the acrylic sediment, particularly at low values of S . The reason may be that curves 7 and 8 in Fig. 3 are upper bounds, as discussed in the next Section.

4. Upper bound and lower bound

So far, we have assumed that the thickness of the mobile layer varies little during the course of a wave cycle and, consequently, it is the average value of the dispersive stress which supports the weight of sediment above. The measurements of Dick and Sleath (1991) showed that this was the situation at very large values of S . At low values of S the sediment settles onto the bed as the flow slows down and then is

eroded again after flow reversal, so there is significant variation in mobile layer thickness during the course of the cycle. Under these circumstances we should use Eq (17) rather than Eq (18).

Most flows show variations in mobile layer thickness during the course of the wave cycle which are somewhere between the two extremes outlined above. Consequently, we should regard curves computed with the aid of Eq (18) as upper bounds and those computed with the aid of Eq (17) as lower bounds. Fig. 4 shows how these upper and lower bound curves compare with the measurements of Li and Sawamoto (1995a) and of Zala Flores and Sleath (1998) with PVC pellets. The upper bound curves are the same as those shown in Fig. 3. We see that the measurements lie between the upper and lower bound curves.

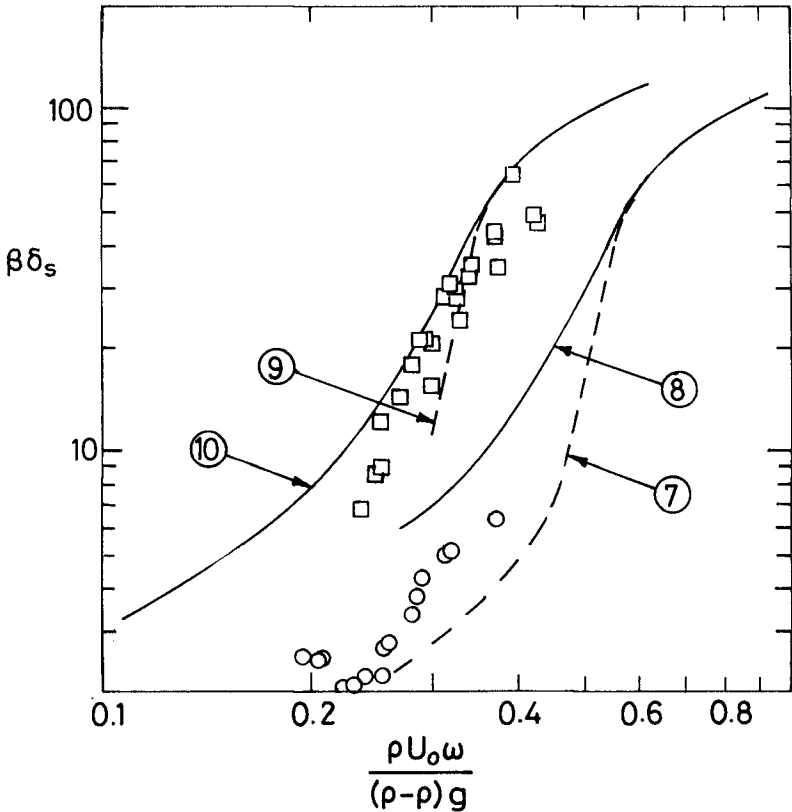


Fig.4 Variation of $\beta\delta_s$ with $\rho U_0 \omega / (\rho_s - \rho)g$. Li and Sawamoto (1995a): O. Zala Flores and Sleath (1998): □ (PVC). Upper bound, Eq (18): curve 7, $V=10$; curve 8, $V=25$. Lower bound, Eq (17): curve 9, $V=10$; curve 10, $V=25$. ($C, K=0.35$, $\theta=12.5^\circ$ in each case).

5. Maximum thickness of mobile layer

The experimental measurements in Figs 1,2,3,4 extend to much larger values of S than those likely to be encountered on site. For example, even under extreme conditions the value of S in the Leman Field in the Southern North Sea does not exceed about 0.2. Madsen's (1974) calculations suggest that a local value of S under the steep forward slope of a near-breaking wave might be as high as 0.36. But, even accepting this higher figure, it would seem from Figs 3 and 4 that the value of $\beta\delta_s$ for beds of sediment on site is unlikely to exceed about 100.

For the Southern North Sea a typical value of wave period for a 50-year storm might be about 13s. With $\beta\delta_s=100$ we obtain $\delta_s \approx 0.2$ m. This value is significantly less than that given by existing empirical formulae for depth of disturbance in the surf zone. For example, the results of King (1951) suggest a depth of disturbance of about 0.5 m for a 50-year storm in the Southern North Sea and Williams' (1971) results lead to even larger values. The most likely explanation for this difference is that the empirical formulae include effects such as the movement of the offshore bar or the migration of sand waves. Clearly, the experimental data and the computations discussed in this paper are for very restricted conditions. The existence of effects such as bed form migration needs to be borne in mind when extending the results to the real world.

6. Conclusions

- (1) Use of the Karman-Polhausen technique makes it possible to calculate parameters of interest without having to assume constitutive equations such as those suggested by Bagnold (1954).
- (2) The calculated curves show good agreement, at high values of S , with existing laboratory measurements of the mobile layer thickness, the phase lead of the velocity at the bottom of the mobile layer, and the ratio of the velocity amplitude and phase scales K_1 / K_2 .
- (3) It is suggested that curves based on the assumption that δ_s is constant during the course of a wave cycle provide an upper bound on the value of S for any given value of $\beta\delta_s$. A lower bound is provided by the assumption that maximum δ_s during the course of a cycle correlates with maximum dispersive stress.
- (4) Although the calculated curves show good agreement with laboratory measurements, the estimates of mobile layer thickness are smaller than the values for depth of disturbance in the surf zone provided by existing empirical formulae. This may be because the present results are for flat beds and, consequently, do not include any allowance for the effects of bed form migration.

Appendix. References

- Asano, T. (1992). Observations of granular-fluid mixture under an oscillatory sheet flow, *Proc. 23rd Conf Coastal Eng.*, ASCE, Reston, Va., 1896-1909.
- Bagnold, R.A. (1954). Experiments on a gravity-free dispersion of large solid spheres in a Newtonian fluid under shear, *Proc. R. Soc. London*, A, 225, 49-63.
- Bagnold, R. A. (1956). The flow of cohesionless grains in fluids, *Phil. Trans. R. Soc. London*, A, 249, 235-297.

- Bakker, W.T., and Van Kesteren, W.G.M. (1986). The dynamics of oscillating sheet flow. *Proc. 20th Conf. Coastal Eng.*, ASCE, Reston, Va., 940-954.
- Dibajnia, M and Watanabe, A. (1992). Sheet flow under nonlinear waves and currents, *Proc. 23rd Conf. Coastal Eng.*, ASCE, Reston, Va., 2015-2028.
- Dick, J.E., and Sleath, J.F.A. (1991). Velocities and concentrations in oscillatory flow over beds of sediment, *J. Fluid Mech.*, 233, 165-196.
- Hanes, D. M., and Inman, D. L. (1985). Observations of rapidly flowing granular-fluid materials, *J. Fluid Mech.*, 150, 357-380.
- Horikawa, K., Watanabe, A., and Katori, S. (1982). Sediment transport under sheet flow conditions, *Proc. 18th Conf. Coastal Eng.*, ASCE, Reston, Va., 1335-1352.
- Jonsson, I.G. (1963). Measurements in the turbulent wave boundary layer, *J. Hydr. Res.*, 14(1), 45-60.
- Kaczmarek, L.M., Ostrowski, R., and Zeidler, R.B. (1995). Boundary layer theory and field bedload, *Proc. Coastal Dynamics 95, Gdansk*, ASCE, Reston, Va., 664-675.
- Katori, S., Mizuguchi, M., and Watanabe, A. (1996). A numerical model of sheet flow sediment transport, *Proc. 25th Conf. Coastal Eng.*, ASCE, Reston, Va., 3818-3829.
- King, C.A.M. (1951). Depth of disturbance of sand on sea beaches by waves, *J. Sed. Petrol.*, 21, 131-140.
- Li, L., and Sawamoto, M. (1995a). Experiments on sediment transport in sheet-flow regime under oscillatory flow, *Coastal Eng. Japan*, 38, 143-156.
- Li, L., and Sawamoto, M. (1995b). Multi-phase model on sediment transport in sheet-flow regime under oscillatory flow. *Coastal Eng. Japan*, 38, 157-178.
- Nadaoka, K., and Yagi, H. (1990). Single-phase fluid modelling sheet-flow toward the development of numerical mobile bed, *Proc. 22nd Conf. Coastal Eng.*, ASCE, Reston, Va., 2346-2359.
- Ono, M., Deguchi, I., and Sawaragi, T. (1996). A numerical model of sheet flow sediment transport, *Proc. 25th Conf. Coastal Eng.*, ASCE, Reston, Va., 3888-3900.
- Ribberink, J. S. and Al-Salem, A. A. (1994). Sediment transport in oscillatory boundary layers in cases of rippled beds and sheet flow. *J. Geophys. Res.*, 99, C6, 12 707-12 727.
- Ribberink, J. S. and Al-Salem, A. A. (1995). Sheet flow and suspension of sand in oscillatory boundary layers, *Coastal Eng.*, 25, 205-225.
- Savage, S.B. and McKeown, S. (1983). Shear stresses developed during rapid shear of concentrated suspensions of large spherical particles between concentric cylinders. *J. Fluid Mech*, 127, 453-472.
- Sawamoto, M., and Yamashita, T. (1986). Sediment transport rate due to wave action, *J. Hydrosci. Hydraul. Eng.*, 4(1), 1-15.
- Schlichting, H. (1979). *Boundary Layer Theory*, 7th ed., McGraw-Hill, New York.
- Sleath, J.F.A. (1994). Sediment transport in oscillatory flow, *Sediment Transport Mechanisms in Coastal Environments and Rivers*, M. Belorgey, R.D. Rajaona, and J.F.A. Sleath, eds., World Scientific, Singapore.
- Williams, A.T. (1971). An analysis of some factors involved in the depth of disturbance of beach sand by waves, *J. Mar. Geol.*, 11, 145-158.
- Zala Flores, N., and Sleath, J.F.A. (1998). Mobile layer in oscillatory sheet flow. *J. Geophys. Res.*, 103, C6, 12 783-12 793.